SCIENCE CHINA
Information Sciences

• RESEARCH PAPER •
July 2020, Vol. 63 170203:1–170203:10
https://doi.org/10.1007/s11432-019-2764-1
Special Focus on Bio-Robotic Systems: Modeling, Design, Control and Perception

A bio-inspired flight control strategy for a tail-sitter unmanned aerial vehicle

Bin ZHU[1], Jianzhong ZHU[2*] & Qingwei CHEN[1]

[1]*Institute of Automation, Nanjing University of Science and Technology, Nanjing* 210094, *China;*
[2]*Department of Energy and Power Engineering, Tsinghua University, Beijing* 100084, *China*

Received 29 September 2019/Accepted 29 November 2019/Published online 29 May 2020

Abstract Wingbeat behavior and intermittent flight path are the two main characteristics of many birds. In this paper, to improve the efficiency of energy use and cruise range, a bio-inspired intermittent flight strategy with a whole flight envelope has applied to a tail-sitter aircraft. A total energy control system based transition control law has been proposed. The energy efficiency is investigated in terms of energy consumption per unit distance of different cruising modes, and the effectiveness and stability of proposed flight mode transition control law are verified by simulation. The mean mechanical power in flap-gliding flight is reduced compared with steady flight.

Keywords tail-sitter aircraft, climb-glide, total energy control system, energy consumption minimization, flight path

Citation Zhu B, Zhu J Z, Chen Q W. A bio-inspired flight control strategy for a tail-sitter unmanned aerial vehicle. Sci China Inf Sci, 2020, 63(7): 170203, https://doi.org/10.1007/s11432-019-2764-1

1 Introduction

Birds, bats, and other flying creatures have been the bio-inspiration source for many novel concepts in the fields of aerodynamic design, flight control, and energy management of aerial vehicles. The flapping-wing micro aerial vehicles (FWAVs) and tail-sitters have become a new development trend in the flying bio-robotic field [1]. In recent years, there have been fruitful FWAV research achievements, not only in terms of the mechanical structure design and aerodynamic model analysis [2], but also in terms of invention of many advanced control methods such as those based on neural networks and learning systems [3–7].

Flying creatures have the capability of adaptability to the environment. For example, some birds can fly at an optimal speed for long distances. In this paper, one of the particular areas of interests is why birds first climb to a high altitude and then glide during the cruise. The reason for such intermittent climb-glide patterns can be that the drag force experienced by birds is much greater than gliding during the propulsion; thus, the climb-glide behavior appears to be an intelligent and optimal approach for energy saving based on animal instinct. These energy minimization strategies have been adopted in the autonomous aerial vehicles to enhance the cruise range and other performance metrics.

The main aim of this study is to investigate the usefulness of bio-inspired energy utilization strategies and flight mode change transition for a tail-sitter unmanned aerial vehicle (UAV). Tail-sitters are capable of vertical takeoff and landing (VTOL), and they can cruise at a very high speed and long endurances like a fixed-wing airplane while retaining the maneuverability and agility of the VTOL [8–11]. Keating [12] discussed four hypotheses to explain the reason why birds adopt the bounding flight. There have been

* Corresponding author (email: jianzhong.zhu@outlook.com)

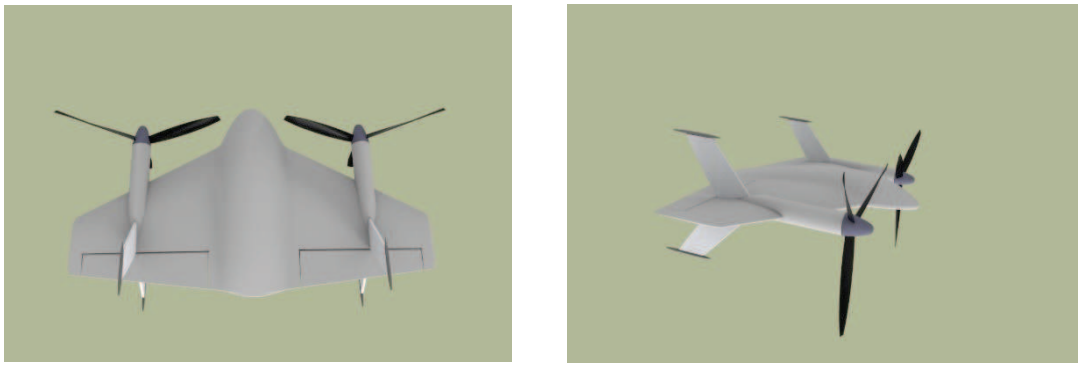

(a) (b)

Figure 1 (Color online) Mechanical structure of the tail-sitter with two motors. (a) Hovering; (b) level flight.

fewer studies on the intermittent climb-glide behavior of aerial vehicles. Trajectory optimization of UAVs [13] and energy minimization of the path design have been analyzed in many studies. For instance, in [14], a comparing thermal soaring with gliding was studied. Wehbe et al. [15] described a dynamic modeling and path planning in the context of energy minimization. Cha et al. [16] considered a high altitude long endurance UAV with a regenerative fuel cell. Four cases of flight paths were tested, and based on the required energy, it was concluded that the climb-glide process represented the most feasible and most energy favorable flight path.

During the flight mode transition, such as changing from climbing to gliding or from hovering to cruising, the horizontal speed of an aircraft can be slower than the cruise speed required for maintaining the altitude, which can result in altitude loss. One of the biggest challenges in tail-sitter development is to solve the problems of altitude loss, performance degradation, and instability during flight mode transitions. The total energy control system (TECS) strategy is an integrated autopilot/autothrottle developed by Boeing, which was experimentally tested by NASA on Boeing 737 aircraft [17]. This system was developed using the principles of total energy in which the total kinetic and potential energy of an airplane is controlled by the throttles while the energy distribution is controlled by the elevator. In 1991, the energy management guidance laws based on the TECS for a high-performance fighter aircraft were proposed by Boeing to coordinate the height/speed transitions to a desired curie point. The coupling of V and γ is resolved in the TECS core by eliminating a functional disharmony between the thrust and flight path control loops [18, 19].

In this paper, to design a long endurance and high energy-efficient flight strategy for a tail-sitter UAV, a detailed dynamic model of a tail-sitter UAV, including the key parameters, longitudinal equations of motion, and aerodynamic forces, is presented. Inspired by the birds flying modes, the whole flight envelope of a tail-sitter UAV with the climb-glide pattern is introduced, and the energy usage of different cruising modes is investigated and compared in terms of energy consumption per unit distance. A TECS strategy for a tail-sitter is proposed and used for attitude stabilization and altitude variation limitation during flight mode transitions within the whole flight envelope.

2 Tail-sitter UAV dynamic modeling

Figure 1 gives an overview of mechanical structure of the developed tail-sitter UAV, which consists of one flying wing with dual rotors and ailerons. The detailed parameters of a tail-sitter are given in Table 1. The hovering control effect of ailerons mainly depends on the dynamic pressure generated by the propeller slipstream.

The main control inputs of an aircraft are the thrust generated by the propeller, and the pitching moment is generated by the ailerons immersed in the slipstream. The differential of the propeller thrust can control the yaw of the aircraft, while the pitch and roll of the aircraft are achieved by the simultaneous or reverse deflection of the two ailerons. For a tail-sitter, the longitudinal equation of motion is expressed

Table 1 Simulation parameters

Parameter	Value	Unit
Wing span b	1.2	m
Wing area S_w	1	m^2
Mean aerodynamic chord c	0.438	m
Efficiency factor e	0.8	–
Parasite drag coefficient C_{D0}	0.025	m
Air density ρ	1.293	kg/m^3
Center of gravity l_w	0.301	m
Moment of inertia I_{yy}	0.04085	$kg \cdot m^2$

as

$$\begin{cases} m(\dot{u}+qw) = L\sin\alpha - D\cos\alpha - mg\sin\theta + T, \\ m(\dot{w}-qu) = -L\cos\alpha - D\sin\alpha + mg\cos\theta, \\ \dot{\theta} = q, \\ \dot{q} = \dfrac{M_y}{I_{yy}}, \\ \dot{X} = u\cos\theta + w\sin\theta, \\ \dot{Z} = -u\sin\theta + w\cos\theta, \end{cases} \tag{1}$$

where u and w denote the body axes velocities; θ and q denote the pitch angle and pitch angular velocity, respectively. α is the angle of attack, T is the thrust of total propellers, and I_{yy} is the moment of inertia. X and Z denote the position of the vehicle in the Earth frame, m and g denote the mass and gravitational acceleration of the tail-sitter, L, D, M_y are the lift and drag aerodynamic forces and pitching aerodynamic moment, respectively, and they are expressed as

$$\begin{cases} L = \dfrac{1}{2}\rho V^2 S_w C_L, \\ D = \dfrac{1}{2}\rho V^2 S_w C_D, \\ M = \dfrac{1}{2}\rho V^2 S_w c C_M, \end{cases} \tag{2}$$

where ρ, V, and S_w are the air density, flight speed, and the wing area, respectively; c denotes the chord length; C_L, C_D, and C_M are the lift force, drag force, and pitching moment coefficients, respectively, and they can be expressed as

$$\begin{cases} C_L = C_{L0} + C_{L\alpha}\alpha + C_{L\delta}\delta + C_{Lq}\dfrac{c}{2V}q, \\ D = C_{D0} + C_{D\alpha}\alpha + C_{D\delta}\delta + C_{Dq}\dfrac{c}{2V}q, \\ M = C_{M0} + C_{M\alpha}\alpha + C_{M\delta}\delta + C_{Mq}\dfrac{c}{2V}q, \end{cases} \tag{3}$$

where δ represents the elevon deflection angle, and it acts as a system control input together with the propeller thrust T.

3 Flight path and control design for tail-sitter UAV

The whole flight envelope of a tail-sitter is shown in Figure 2. During the taking-off and landing procedures, the propellers produce lift, so the tail-sitter flies as a rotary-wing aircraft. In the transition process, the aircraft pitches downward or upward so that it can change flight mode from hovering to cruise, and vice versa. When cruising at horizontal flight stage, it flies as a fixed-wing aircraft, and the lift is produced by the aerodynamic force, thus allowing a longer endurance.

When a vehicle starts to climb to the desired altitude, the pitch and thrust coordinate controllers take charge during the transition process. In general, the transition control scheme consists of two parts [20].

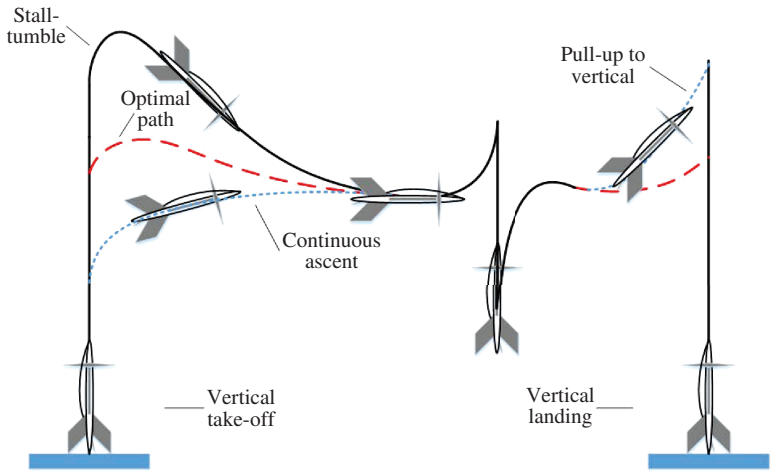

Figure 2 (Color online) The whole flight envelope of the tail-sitter.

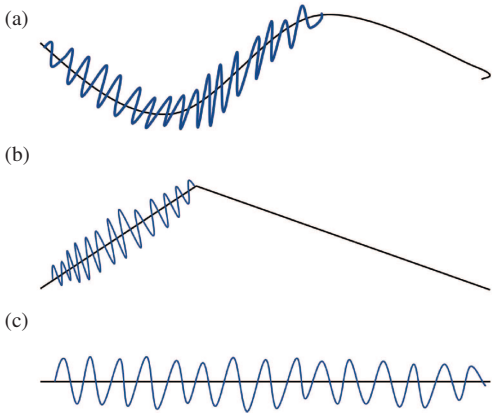

Figure 3 (Color online) Intermittent biomimetic flight strategies observed with birds (from Rayner). (a) Bounding (flap-bounding); (b) undulating (flap-gliding); (c) chattering.

The first part is the trajectory or the strategy for the transition process. There are three common themes shown in the Figure 2 for the trajectory objective: stall-tumble, optimal path [21, 22], and continuous ascent [23–25]. The second is the controller. Because the control inputs are thrust and the pitch angle caused by the slip flow, the flight speed, and height of a vehicle cannot be controlled simultaneously. In order to maintain an aircraft to obtain sufficient flight speed under the condition of small change in altitude during the transition mode, the coordinated control of the longitudinal attitude is required.

3.1 Intermittent flight strategy for tail-sitter UAV

The manner in which the tail-sitter completes the front transition and the manner of its stall-tumble and optimal path can be considered as types of climb-glide behaviors. By considering the energy consumption minimization and long endurance of a tail-sitter, a strategy of intermittent burst-coast and climb-glide for horizontal flight stage is proposed in this paper.

The intermittent strategies, involving the bounding, undulating, and chattering flight patterns, which have been observed with birds are presented in Figure 3 [26,27]. In this paper, the intermittent biomimetic flight strategy is applied to a tail-sitter UAV for a long enduring purpose. Figure 3(a) is not suitable because the flight trajectory can difficultly achieve sine shape. The undulating strategy presented in Figure 3(b) is considered. The idea of energy arrangement is that the thrust is set as maximum in the climb stage, and for the gliding part, elevator is the only way to control the attitude. The energy required for the whole process is calculated and compared with Figure 3(c) wherein a vehicle flies at a continuous level.

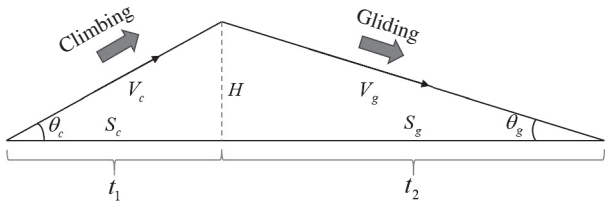

Figure 4 Undulating flight strategy.

3.2 Energy consumption

In this subsection, the power consumptions of a level flight and an intermittent flight of a UAV are calculated [16]. In the calculation process, a circle or spiral flight and influence of the winds is ignored. The corresponding equations of motions are functions of air density ρ, weight m, lift coefficient C_L, drag coefficient C_D, and wing area S_w, where T is the thrust required to obtain a certain steady velocity. For a level flight, the equation of motion is expressed as

$$T = D = m\frac{C_D}{C_L}, \tag{4}$$

$$L = m = \frac{1}{2}\rho V^2 S_w C_L, \tag{5}$$

$$D = \frac{1}{2}\rho V^2 S_w C_D, \tag{6}$$

and the required power is given by

$$P_l = TV_l = \sqrt{\frac{2m^3 C_D^2}{\rho S_w C_L^3}}. \tag{7}$$

Figure 4 shows the two phases of climb-glide flight. For the climbing flight phase, the influence of the winds is ignored. Namely, it is considered that the attacking angle of an aircraft is relatively small, so the pitch angle θ can be approximated to γ, and the equation of motion and the required energy can be expressed as

$$T = D + m\sin\theta_c, \tag{8}$$

$$L = m\cos\theta_c = \frac{1}{2}\rho V_c^2 S_w C_L, \tag{9}$$

$$P_c = DV_c + mV_c\sin\theta_c. \tag{10}$$

For the gliding flight, the equation of motion is given by

$$L = m\cos\theta_g = \frac{1}{2}\rho V_g^2 S_w C_L, \tag{11}$$

and the velocity is expressed as

$$V_g = \sqrt{\frac{2m\cos\theta_g}{\rho S_w C_L}}. \tag{12}$$

During the gliding flight phase, the tail-sitter does not consume any energy. Therefore, the energy consumed by the two flight modes is given by

$$\begin{cases} P_l = \sqrt{\dfrac{2m^3 C_D^2}{\rho S_w C_L^3}}, \\ P_c = DV_c + mV_c\sin\theta_c. \end{cases} \tag{13}$$

3.3 Total energy control for climb-glide flight

The TECS approach was first introduced by Lambregts [13] to control the longitudinal dynamics of a fixed wing aircraft. The main ideas are to use the throttle to control the energy and to use the flight-path angle to control the energy distribution between height and speed requirements. The TECS algorithm is based on the following principles and assumptions.

Assumption 1. The kinetic energy and potential energy can be transformed into each other, so as the relationship between height and speed.

Assumption 2. Suppose the aircraft is a rigid body, its motion is particle motion, and aircraft thrust and flight resistance are the only ways to generate and offset energy.

Assumption 3. It is considered that the attacking angle of an aircraft is relatively small, and the influence on the drag caused by a change in the flight-path angle is negligible. The aircraft dynamic can be expressed using the energy states as

$$E_T = E_k + E_p = \frac{1}{2}mV^2 + mgH, \tag{14}$$

where E_k denotes the kinetic energy, and E_p denotes the potential energy. By differentiating (14), the unit energy rate can be obtained as follows:

$$\dot{E} = V\left(\frac{\dot{V}}{g} + \gamma\right). \tag{15}$$

Assume E_e is the total energy deviation and $\dot{E}_e$ is the deviation of the total energy change rate of an aircraft. Then it can be written as

$$\dot{E}_e = \left(\frac{\dot{V}_e}{g} + \gamma_e\right), \tag{16}$$

$$\dot{V}_e = \dot{V}_c - \dot{V}, \tag{17}$$

$$\gamma_e = \gamma_c - \gamma. \tag{18}$$

The amount of the total energy rate is influenced by inputs through different thrust, so the controller can be expressed as

$$T_{\text{cmd}} = \left(K_{tp} + \frac{K_{ti}}{s}\right)\dot{E}_e. \tag{19}$$

According to the definition of total energy, the energy distribution can be expressed as

$$L_d = E_p - E_k = mgH - \frac{1}{2}mV^2. \tag{20}$$

Next, define L_e as the energy distribution deviation, and $\dot{L}_e$ as the energy distribution rate deviation:

$$\dot{L}_e = \left(\gamma_e - \frac{\dot{V}_e}{g}\right). \tag{21}$$

The changes in pitch attitude lead to the energy redistribution, where the elevator control plays the role of a conservative energy distributor.

$$\theta_{\text{cmd}} = \left(K_{dp} + \frac{K_{di}}{s}\right)\dot{L}_e. \tag{22}$$

Therefore, the main principle of the TECS can be expressed as follows:

$$\begin{cases} T_{\text{cmd}} = \left(K_{tp} + \dfrac{K_{ti}}{s}\right)\dot{E}_e, \\ \theta_{\text{cmd}} = \left(K_{dp} + \dfrac{K_{di}}{s}\right)\dot{L}_e. \end{cases} \tag{23}$$

The feedback proportion gains K_{tp}, K_{dp} and integration parameters K_{ti}, K_{di} are tuned to yield dynamics of $\dot{E}_e$ and $\dot{L}_e$. In the TECS, the thrust and elevator control the coordination in a decoupled response, which makes the flight path angle command have a negligible influence on speed fluctuation, and vice versa [28].

The classic TECS core is a steady state error control of flight speed and altitude. In (16), when $\dot{E}_e = 0$, the flight path angel and speed rate deviation are equal to zero ($\gamma_e = \dot{V}_e = 0$), but the speed deviation differs from zero ($V_e \neq 0$). In order to eliminate the speed steady error, an equivalent control for $\dot{V}_c$ has been used:

$$\dot{V}_c = K_v(V_c - V). \tag{24}$$

Eq. (17) can then be rewritten as $\dot{V}_e = \dot{V}_c - \dot{V} = K_v(V_c - V) - \dot{V}$, and $V_c = V$ when $\dot{V}_e = 0$. However, using V_e instead of $\dot{V}_c$ will lose the acceleration control information, which makes the control slow. In order to solve this problem, the speed deviation control is introduced. The deviation of the total energy change rate given by (16), and deviation of the energy distribution rate given by (21) can be respectively rewritten as

$$\begin{cases} \dot{E}_{ev} = \gamma_e + \dfrac{\dot{V}_e}{g} + K_v(V_c - V), \\ \dot{L}_{ev} = \gamma_e - \dfrac{\dot{V}_e}{g} - K_v(V_c - V). \end{cases} \tag{25}$$

Because $\gamma_e = \dot{H}_e/V$, the altitude error will differ from zero when $\gamma_e = 0$. By using an equivalent control for $\dot{H}_c$, and adding the altitude deviation as $\Delta H = K_h(H_c - H)$, the feedback of flight path angle deviation can be rewritten as

$$\gamma'_e = \frac{\dot{H}_e + \Delta H}{V}. \tag{26}$$

By combining (25) and (26), we get

$$\begin{cases} \dot{E}_{\text{evh}} = \gamma'_e + \dfrac{\dot{V}_e}{g} + K_v V_e, \\ \dot{L}_{\text{evh}} = \gamma'_e - \dfrac{\dot{V}_e}{g} - K_v V_e. \end{cases} \tag{27}$$

Then, the improved TECS can be expressed as

$$\begin{cases} T_{\text{cmd}} = K_{tp}\dot{E} + \dfrac{K_{ti}}{s}\dot{E}_{\text{evh}}, \\ \theta_{\text{cmd}} = K_{dp}\dot{L} + \dfrac{K_{di}}{s}\dot{L}_{\text{evh}}. \end{cases} \tag{28}$$

In (28), the total energy rate and distribution rate are used instead of the energy error rate because the energy error rate as being a derivative term will bring significant oscillation. The improved TECS scheme is illustrated in Figure 5.

4 Simulation

In order to compare the energy consumed by a continuous steady level flight with that consumed by a climb-glide flight, the targeted altitude of an undulating flight is set to 1200 m. The improved TECS is used to control the altitude and speed during the climb phase. The aerial dynamic of the tail-sitter UAV is a 3-DOF (three degrees of freedom) equation.

The energy consumed by the two flight modes is given by

$$\begin{cases} P_l = \sqrt{\dfrac{2m^3 C_D^2}{\rho S_w C_L^3}}, \\ P_c = DV_c + mV_c \sin\theta_c. \end{cases} \tag{29}$$

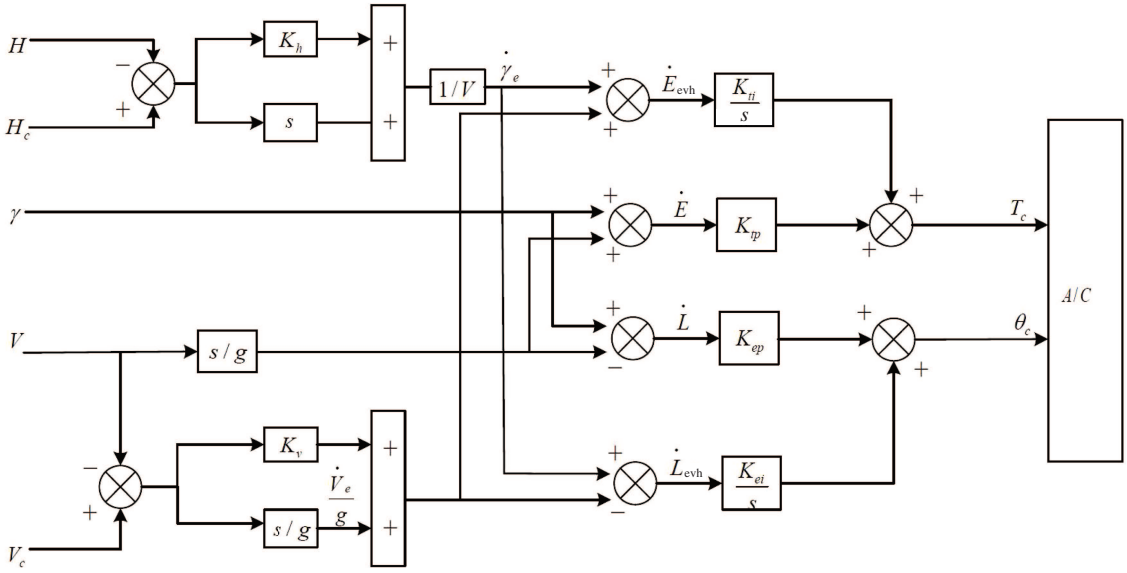

Figure 5 Improved TECS control scheme.

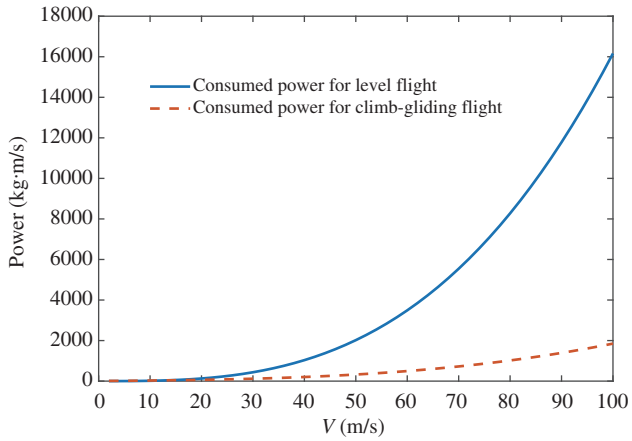

Figure 6 (Color online) Energy consumed by the two flight modes.

Based on (5), the lift coefficient is calculated by

$$C_L = \frac{m}{\frac{1}{2}\rho V^2 S_w}. \tag{30}$$

The drag coefficient from the known drag polar of the airplane is given by

$$C_D = C_{D0} + \frac{C_L^2}{\pi e AR}, \tag{31}$$

where parameter e denotes the efficiency factor, C_{D0} denotes the parasite drag coefficient, and $AR = b^2/S_w$. By substituting (30) and (31) into (29), the energy consumed by the level flight and climb-gliding flight modes at different velocity is calculated, and the obtained results are shown in Figure 6.

As shown in Figure 6, the energy consumed during the level flight is much higher than that consumed by the climb-glide flight strategy proposed in this paper. As the speed increases, more energy is consumed; when the speed reaches the value of 100 m/s, the energy consumed in the horizontal flight mode is 8 times larger than that in the climb-glide flight mode. This is because as the speed increases, the drag force increases significantly, which requires more energy to overcome the drag in the horizontal flight mode.

In the intermittent flight pattern, the vehicle needs to climb and glide many times. When the vehicle starts to climb to the desired altitude, the pitch and thrust coordination controllers take charge in the

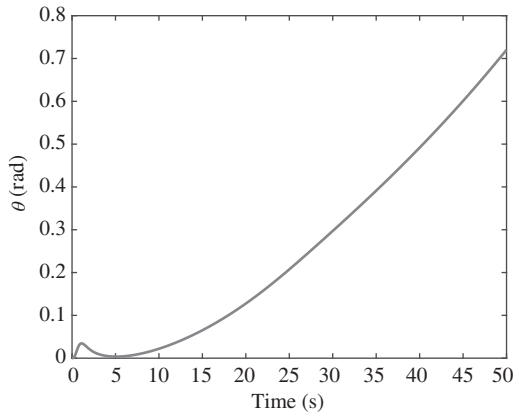

Figure 7 θ of climb phase.

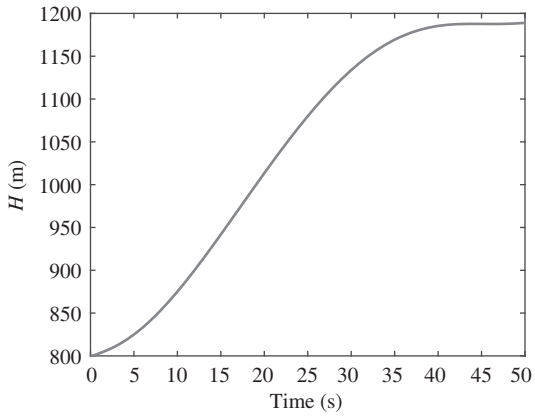

Figure 8 Trajectory of climb phase.

transition process. As shown in Figures 7 and 8, by applying the proposed controller, the aircraft could change the flight mode and reach the target altitude smoothly. The final error level could be further improved by tuning the controller gains.

5 Conclusion

In this paper, a bio-inspired intermittent flight strategy for a tail-sitter UAV was proposed to enhance energy efficiency and address long endurance. The undulating flight includes the climb phase and glide phase, and the tail-sitter requires power only for the climb phase. A whole flight envelope including different flight modes is introduced, and a bio-inspired climb-glide intermittent flight pattern is used to minimize the energy consumption during the cruising process. The effectiveness of the proposed strategy is verified by simulations, analyzing the level flight in terms of energy consumption per unit travel distance. In order to ensure the stability and smoothness during the flight mode transition, an improved transition control law based on the TECS is designed. Simulation results show that by using the proposed control strategy, the aircraft can converge to the desired values smoothly.

References

1 He W, Huang H F, Chen Y N, et al. Development of an autonomous flapping-wing aerial vehicle. Sci China Inf Sci, 2017, 60: 063201
2 Yin D F, Zhang Z S. Design, fabrication and kinematics of a bio-inspired robotic bat wing. Sci China Tech Sci, 2016, 59: 1921–1930
3 He W, Meng T, He X, et al. Iterative learning control for a flapping wing micro aerial vehicle under distributed disturbances. IEEE Trans Cybern, 2019, 49: 1524–1535
4 Zhang S, Dong Y, Ouyang Y, et al. Adaptive neural control for robotic manipulators with output constraints and uncertainties. IEEE Trans Neural Netw Learn Syst, 2018, 29: 5554–5564
5 Zhang S, Yang P, Kong L, et al. Neural networks-based fault tolerant control of a robot via fast terminal sliding mode. IEEE Trans Syst Man Cybern Syst, 2019. doi: 10.1109/TSMC.2019.2933050
6 He W, Zhang S. Control design for nonlinear flexible wings of a robotic aircraft. IEEE Trans Contr Syst Technol, 2017, 25: 351–357
7 He W, Dong Y. Adaptive fuzzy neural network control for a constrained robot using impedance learning. IEEE Trans Neural Netw Learn Syst, 2018, 29: 1174–1186
8 Wang W F, Zhu J H, Kuang M C, et al. Design and hovering control of a twin rotor tail-sitter UAV. Sci China Inf Sci, 2019, 62: 194202
9 Osborne S R. Transitions between hover and level flight for a tailsitter UAV. Dissertation for Master's Degree. Provo: Brigham Young University, 2007
10 Kubo D, Suzuki S. Tail-sitter vertical takeoff and landing unmanned aerial vehicle: transitional flight analysis. J Aircraft, 2008, 45: 292–297
11 Jung Y, Shim D H. Development and application of controller for transition flight of tail-sitter UAV. J Intell Robot Syst, 2012, 65: 137–152
12 Keating H A. A Literature Review on Bounding Flight in Birds With Applications to Micro Uninhabited Air Vehicles. DSTO-GD-0320, 2002

13 Bai T T, Wang D B. Cooperative trajectory optimization for unmanned aerial vehicles in a combat environment. Sci China Inf Sci, 2019, 62: 010205
14 Ákos Z, Nagy M, Leven S, et al. Thermal soaring flight of birds and unmanned aerial vehicles. Bioinspir Biomim, 2010, 5: 045003
15 Wehbe B, Shammas E, Zeaiter J, et al. Dynamic modeling and path planning of a hybrid autonomous underwater vehicle. In: Proceedings of IEEE International Conference on Robotics & Biomimetics, 2015
16 Cha M Y, Kim M, Sohn Y J, et al. Flight paths for a regenerative fuel cell based high altitude long endurance unmanned aerial vehicle. J Mech Sci Technol, 2016, 30: 3401–3409
17 Bruce K R, Kelly J R, Person J L H. NASA B737 flight test results of the total energy control system. In: Proceedings of AIAA Guidance, Navigation and Control Conference, Williamsburg, 1986
18 Wu S F, Guo S F. Optimum flight trajectory guidance based on total energy control of aircraft. J Guid Control Dyn, 1994, 17: 291–296
19 Lambregts A A. TECS Generalized Airplane Control System Design—An Update, Advances in Aerospace Guidance, Navigation and Control. Berlin: Springer, 2013
20 Argyle M E. Modeling and control of a tailsitter with a ducted fan. Dissertation for Ph.D. Degree. Provo: Brigham Young University, 2016
21 Maqsood A, Go T H. Optimization of hover-to-cruise transition maneuver using variable-incidence wing. J Aircraft, 2010, 47: 1060–1064
22 Maqsood A, Go T H. Transition maneuver of a small unmanned air vehicle using aerodynamic vectoring. In: Proceedings of 2011 Defense Science Research Conference and Expo (DSR), Singapore, 2011. 1–4
23 Jung Y D. A multimodal flight control design and flight test of a tail-sitter UAV. Dissertation for Ph.D. Degree. Taejon: Korea Advanced Institute of Science and Technology, 2014
24 Jung Y, Shim D H, Ananthkrishnan N. Controller synthesis and application to hover-to-cruise transition flight of a tail sitter UAV. In: Proceedings of AIAA Atmospheric Flight Mechanics Conference, 2010. 1–24
25 Kita K, Konno A, Uchiyama M. Transition between level flight and hovering of a tail-sitter vertical takeoff and landing aerial robot. Adv Robot, 2010, 24: 763–781
26 Rayner J M V. The intermittent flight of birds. In: Scale Effects in Animal Locomotion. London: Academic Press, 1977. 437–443
27 Rayner J M V, Swaddle J P. Aerodynamics and behaviour of moult and take-off in birds. In: Biomechanics and Behaviour. London: Bios Publishers, 2000
28 Chudy P, Rzucidlo P. TECS/THCS based flight control system for general aviation. In: Proceedings of AIAA Modeling and Simulation Technologies Conference, Chicago, 2009